The Journal of Experimental Biology 216, 407-417

doi:10.1242/jeb.074658

RESEARCH ARTICLE

Mechanics of snout expansion in suction-feeding seahorses: musculoskeletal force transmission

Sam Van Wassenbergh[1,*], Heleen Leysen[2], Dominique Adriaens[2] and Peter Aerts[1,3]

[1]Department of Biology, Universiteit Antwerpen, Universiteitsplein 1, B-2610 Antwerp, Belgium, [2]Evolutionary Morphology of Vertebrates, Ghent University, K. L. Ledeganckstraat 35, B-9000 Ghent, Belgium and [3]Department of Movement and Sports Sciences, Ghent University, Watersportlaan 2, B-9000 Ghent, Belgium

*Author for correspondence (sam.vanwassenbergh@ua.ac.be)

SUMMARY

Seahorses and other syngnathid fishes rely on a widening of the snout to create the buccal volume increase needed to suck prey into the mouth. This snout widening is caused by abduction of the suspensoria, the long and flat bones outlining the lateral sides of the mouth cavity. However, it remains unknown how seahorses can generate a forceful abduction of the suspensoria. To understand how force is transmitted to the suspensoria *via* the hyoid and the lower jaw, we performed mathematical simulations with models based on computerized tomography scans of *Hippocampus reidi*. Our results show that the hinge joint between the left and right hyoid bars, as observed in *H. reidi*, allows for an efficient force transmission to the suspensorium from a wide range of hyoid angles, including the extremely retracted hyoid orientations observed *in vivo* for syngnathids. Apart from the hyoid retraction force by the sternohyoideus–hypaxial muscles, force generated in the opposite direction on the hyoid by the mandibulohyoid ligament also has an important contribution to suspensorium abduction torque. Forces on the lower jaw contribute only approximately 10% of the total suspensorium torque. In particular, when dynamical aspects of hyoid retraction are included in the model, a steep increase is shown in suspensorium abduction torque at highly retracted hyoid positions, when the linkages to the lower jaw counteract further hyoid rotation in the sagittal plane. A delayed strain in these linkages allows syngnathids to postpone suction generation until the end of cranial rotation, a fundamental difference from non-syngnathiform fishes.

Key words: prey capture, Syngnathidae, biomechanics.

Received 4 May 2012; Accepted 19 September 2012

INTRODUCTION

Many aquatic vertebrates use suction, generated *via* expansion of the buccopharyngeal cavity, to capture their prey. This expansion quickly draws a certain volume of water (and any prey failing to escape) into the mouth. In actinopterygian fishes, buccopharyngeal expansion typically occurs simultaneously in the dorsoventral and lateral direction (e.g. Sanford and Wainwright, 2002). Dorsoventral expansion is generated by displacing the floor and the roof of the mouth cavity away from each other. Examples of fish that almost uniquely rely on dorsoventral expansion are clariid catfish, in which the rotation of the lower jaw, hyoid and pectoral girdle causes the tips of these three arched elements to push down on the ventral tissues of the mouth cavity (Van Wassenbergh et al., 2007a).

However, in contrast to the levers and linkages involved in these ventral rotations, which have been studied extensively in the past decades (e.g. Muller, 1987; Muller, 1996; Westneat, 1994; Waltzek and Wainwright, 2003; Roos et al., 2009a; Ferry-Graham and Konow, 2010), relatively little is known about the mechanics of lateral expansion. Lateral expansion occurs by abduction of the bony elements covering the sides of the head in actinopterygian fish. These elements are the suspensoria (a complex of several viscerocranial bones from the mandibular and hyoid arches) and the opercula (the bones covering the gills).

The abduction of the suspensoria has especially been recognized as an indispensable tool in powering suction, for example in cichlid fishes (Aerts, 1991; Aerts and Verraes, 1991; De Visser and Barel, 1996; De Visser and Barel, 1998). Suspensorium abduction can best be visualized as two doors (the left and right suspensorial planes) suspended from two rostrad converging rotation axes attached to a ceiling (the ventral neurocranial surface) (De Visser and Barel, 1996). The simplest view is that the suspensoria 'suspend' two pairs of converging rods at their ventral side: the left and right hyoid bars and the left and right lower jaw elements. Due to the articulation of the hyoid with the suspensoria, changes in the abduction–adduction angle of the suspensoria are coupled with changes in the angles between the left and right hyoids and lower jaws. Note, however, that the suspension of the hyoid can sometimes be more complex in fish, including additional joints formed by the simplectic and interhyal bones (e.g. Gregory, 2002).

Despite this essential role of the suspensoria during suction feeding in fish, it is still partly unclear how fish manage to transmit sufficient force to perform a forceful and powerful suspensorial abduction. There is a muscle (levator arcus palatini) that can generate suspensorium abduction torque directly. However, all authors that have studied the function of this muscle using mathematical modelling agree that, due to its small size and its unfavourable line of action for inducing torque, the role of the levator arcus palatini during suction feeding is negligible, and that force has to be transmitted *via* the hyoid (Muller, 1989; Aerts, 1991; Aerts and Verraes, 1991; De Visser and Barel, 1996; De Visser and Barel,

1998). The muscles powering retraction of the hyoid (sternohyoideus, hypaxial and epaxial muscles) are several orders of magnitude larger in volume compared with the levator arcus palatini. Manipulation of fresh specimens of almost any suction-feeding ray-finned fish shows that hyoid retraction results in outward motion of the suspensoria.

However, the force transmission from hyoid retraction to suspensorium abduction depends strongly on the nature of the joint at the symphysis between the left and right hyoid bars (Aerts, 1991). This symphysis is also the location where the hyoid retraction input force is applied. The joint at the hyoid symphysis has traditionally been modelled as a spherical joint (Muller, 1989; De Visser and Barel, 1996), but Aerts recognized that for the cichlid species *Haplochromis elegans*, a hinge joint more accurately corresponds to the morphology of the animal, which showed connective tissue along an axis at the hyoid symphysis on stained histological sections (Aerts, 1991). The same study also pointed out that not only the hyoid retraction input force vector should be considered, but also the anterior directed forces on the hyoid from linkages to the lower jaw. Furthermore, the role of the lower jaw in this process, which is also forcefully retracted (i.e. experiencing a posteriorly directed force) during mouth opening and connects *via* ball-and-socket joints to the suspensoria, has not been studied thus far. Consequently, the mechanics of lateral buccopharyngeal expansion in fish remain poorly understood.

Seahorses (and other syngnathid species like pipefish) rely entirely on suspensorial abduction to generate suction (Roos et al., 2009b). The sides of the relatively long snout of a seahorse are formed by elongated suspensoria (e.g. Branch, 1966; Leysen et al., 2010; Leysen et al., 2011). After rotating the head and bringing the mouth close to the prey (Van Wassenbergh and Aerts, 2008; Roos et al., 2009b), widening of the snout generates a sufficient volume increase of the mouth cavity to successfully draw small crustaceans through the expanding snout. However, their relatively small hyoid shows a rotation magnitude that is abnormally large for fish: it regularly rotates over 120 deg with respect to the snout axis (Roos et al., 2009b). A high-speed video analysis of prey capture in *Hippocampus reidi* showed that most of the snout widening occurs when the hyoid tip is pointing posteriorly (i.e. having rotated over 90 deg) (Fig. 1). With the hyoid in such a posture, a posterior force along the sternohyoid line of action combined with a spherical joint at the hyoid symphysis would cause suspensorial adduction instead of abduction. Consequently, we hypothesize that, similar to *H. elegans* (Aerts, 1991), the hyoid symphysis will function as a hinge joint, thereby extending the hyoid rotation range over which further buccopharyngeal expansion can be generated.

The central aim of this study is to unravel how suction is powered in seahorses, where dorsoventral expansion is absent, and suction generation is driven entirely by suspensorium abduction. Does the hyoid symphysis in syngnathids function as a hinge joint (*sensu* Aerts, 1991; de Lussanet and Muller, 2007) or as a spherical (i.e. synovial or ball-and-socket) joint (*sensu* Muller, 1989; De Visser and Barel, 1996)? Finally, what is the role during suction generation of the ligaments, tendons and muscles linking the hyoid to the lower jaw? To answer these questions, force transmission for suspensorial motion *via* the hyoid and the lower jaw will be analysed by mathematical modelling, including multiple rigid elements and joints.

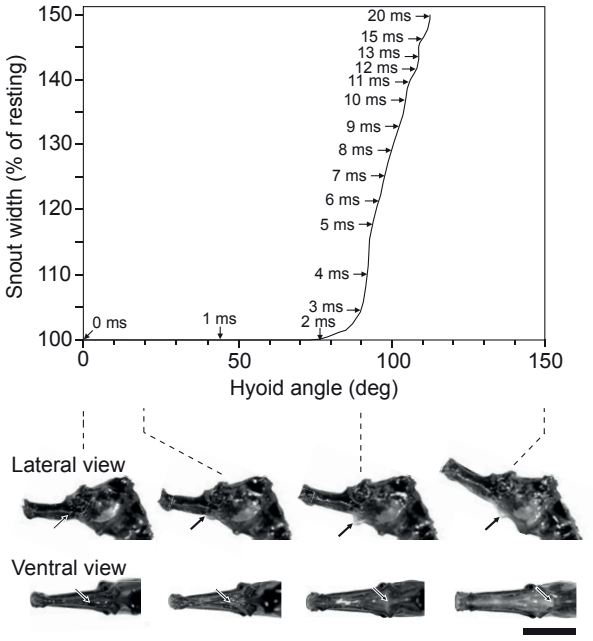

Fig. 1. Relationship between the position of the hyoid during feeding (angle with respect to the snout axis) and the width of the snout in *Hippocampus reidi*, as quantified by Roos et al. (Roos et al., 2009b) using high-speed video. Time is indicated by the labelled arrows on the curve. The pictures below illustrate the position of the hyoid (tip marked by arrows) in lateral and ventral views (manipulated specimen). Note that snout widening starts after the hyoid is retracted further than 80 deg, and widening continues gradually while the hyoid is relatively slowly retracted further to ~115 deg. Scale bar, 10 mm.

MATERIALS AND METHODS

Bony elements and joint morphology

The geometry of the left and right suspensoria, ceratohyals and lower jaws were included as rigid elements in the model (Fig. 2A). This geometry was based on a computerized tomography (CT) scan of our model species *Hippocampus reidi* Ginsburg 1933, of which three-dimensional (3D) reconstructions were generated and used previously in a morphological study (Leysen et al., 2011). This scan was taken at the micro-CT setup of Ghent University, Belgium (UGCT). The standard length and head length of the scanned specimen were 119.0 and 25.2 mm, respectively. Prior to scanning, at the fixation stage, the specimen was forced into an adducted position so that the hyoid and suspensorium position approximates the posture at the onset of feeding.

A Standard Tessellation Language export of the 3D reconstruction of the scan was imported into VRMesh Studio 5.0 software (VirtualGrid, Bellevue City, WA, USA), and aligned to an orthogonal co-ordinate system with the *x*-axis defined as the right–left axis, the *y*-axis as the ventral–dorsal axis, and the *z*-axis as the posterior–anterior axis (Fig. 2). The 3D co-ordinates of the 12 anatomical landmarks required to define the positions and hinge axes orientations of the model were determined (Fig. 2B; a detailed list of the specific landmarks is provided in the legend of this figure).

A closer inspection of the symphysis region of the ceratohyals indicated that, as expected, a hinge joint captures the morphology more precisely than a joint with more degrees of freedom such as a spherical (ball-and-socket) joint. The CT scan showed a contacting ridge between the ceratohyals of about half the total length of the ceratohyals (Fig. 2D). The available serial histological sections of this species (Leysen et al., 2011) confirmed this by showing a series of connective tissue bridges between the left and right elements at this approximately linear contact zone. A comparable situation was found for the lower jaws (Fig. 2D) where the anterior ends of the left and right dentaries are not connected at a single point, but in a

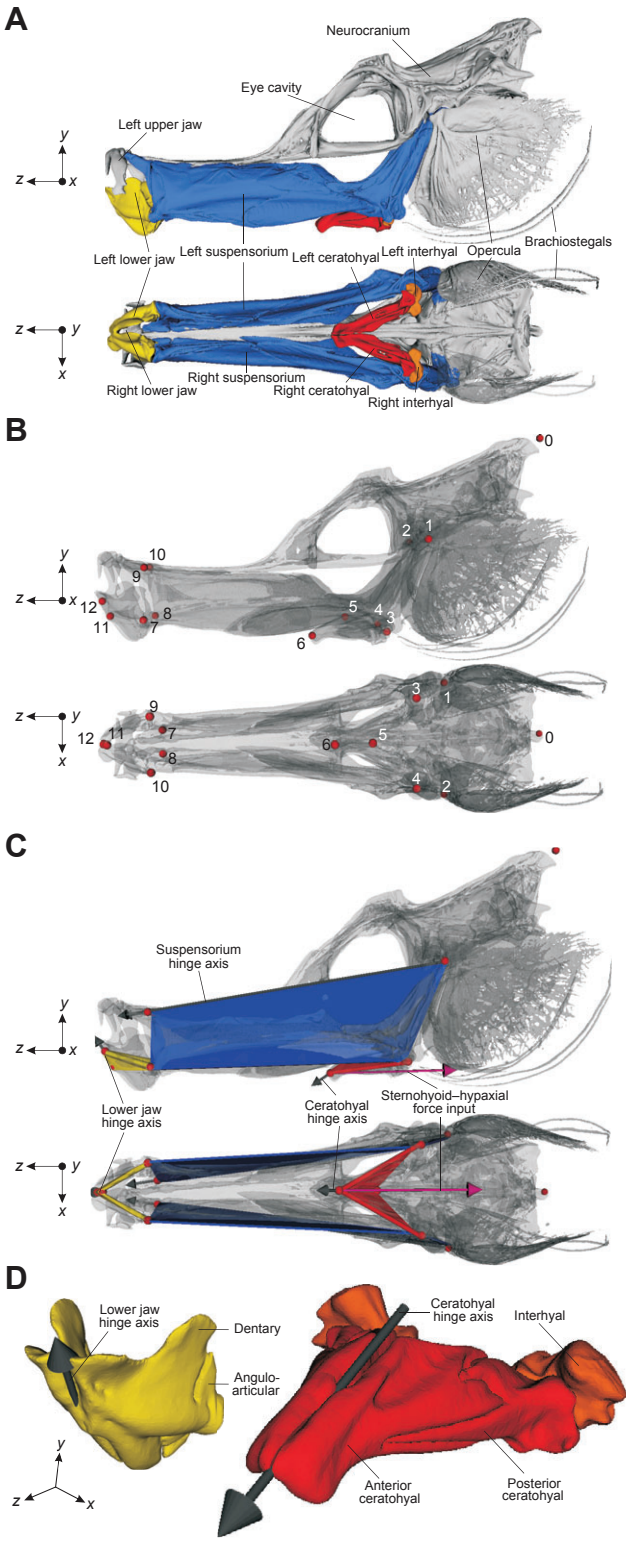

Fig. 2. Determination of the model geometry based on CT scan reconstructions of *Hippocampus reidi* (Leysen et al., 2011). The original scan (A) is shown with colour coding of the main elements involved in mouth cavity expansion: the lower jaws (yellow), the suspensoria (blue), the ceratohyals (red), and the interhyal (orange). 3D positions of the points used for constructing the model are illustrated in B: (0) model origin near the coronet, (1) left and (2) right joint connection of the hyomandibula and the pterotic bones, (3) left and (4) right centres of the interhyals, (5) posterior-most medial contact point between left and right ceratohyals, (6) symphysis of the ceratohyals, (7) left and (8) right joints between the lower jaw (angulo-articular) and the suspensoria (quadrate), (9) left and (10) right joint connections of the quadrate and the antorbital bone, (11) posterior-most medial contact point between left and right anterior ridges of the dentaries, and (12) symphysis of the dentaries. Schematic representation of the model (C) showing the orientation of the four hinge axes and four spherical joints, as well as the input force vector for hyoid retraction by the sternohyoideus–hypaxial muscle complex. An enlarged view on the lower jaws (left) and hyoids (right) (D) gives a more detailed view on the two medial hinge axes of the model.

larger, elongated zone. Therefore, it was decided to model the lower jaw symphysis as a hinge joint as well. Note, however, that the orientation of the hinge axes of the ceratohyal and dentary symphysis differ considerably in *H. reidi* (Fig. 2).

Although articulations between dentaries and anguloarticulars (Aerts et al., 1987; Vial and Ojeda, 1992; Konow et al., 2008; Ferry-Graham and Konow, 2010), and between the anterior and posterior ceratohyals of a single side (Diogo, 2005; Adriaens et al., 2010) are relatively common in actinopterygian fishes, the model assumes that mobility in these connections is negligible in *H. reidi*. The posterior ceratohyal bone tapers ventrally where there is a strongly interdigitated, firm synchondrosis with the anterior ceratohyal bone (Leysen et al., 2011). Since this connection leaves virtually no freedom of movement, the ceratohyal parts of a single side can safely be regarded as a rigid unit. The angular and dentary bones, however, are not very firmly interdigitated in *H. reidi* (Leysen et al., 2011). This allows for some torsion along the long axis (*sensu* Aerts et al., 1987). A notable intra-mandibular flexion in the sagittal plane, however, was not observed in syngnathids (Van Wassenbergh et al., 2008; Roos et al., 2009b; Van Wassenbergh et al., 2011).

Linkage morphology

Three paired linkages connect the hyoid (ceratohyals) to the lower jaw: (1) the left and right mandibulohyoid ligaments, (2) the protractor hyoidei muscle and associated left and right tendons, and (3) the left and right interopercular bones and associated ligaments (Fig. 3). Close to the hyoid, the cross-sectional area of a protractor hyoidei tendon and an interopercular ligament are, respectively, 5 and 22% of the cross-sectional area of a mandibulohyoid ligament [measured by fitting ellipses on serial histological section images from the study of Leysen et al. (Leysen et al., 2011); Fig. 3B]. Consequently, the mandibulohyoid ligaments are much thicker in cross-section compared with the tendons and ligaments of the other two linkages.

The origin of the mandibulohyoid ligaments is relatively close to the hyoid symphysis, at ~70% of the hyoid length measured from the interhyal centre to the most distal point on the ceratohyal (Fig. 3A). Their attachments on the ceratohyals are considerably more medial compared with the other linkages (Fig. 3). From its ceratohyal origin, the mandibulohyoid ligament runs almost parallel with the ceratohyals, makes a curve when approaching the base of the ceratohyals, and then runs in a straight line to a ventromedial insertion on the left and right dentaries. When the hyoid is in its adducted state (i.e. ceratohyal tips pointing rostrally), the mandibulohyoid ligament is folded completely at the dorso-posterior region of the ceratohyals. When the hyoid is retracted, the angle of this ‘fold’ is gradually straightened (Fig. 3A).

The protractor hyoidei muscle is attached *via* tendons at the lateral sides of the left and right ceratohyals, close to the interhyals (Fig. 3A). Running anteriorly, these relatively thin tendons converge

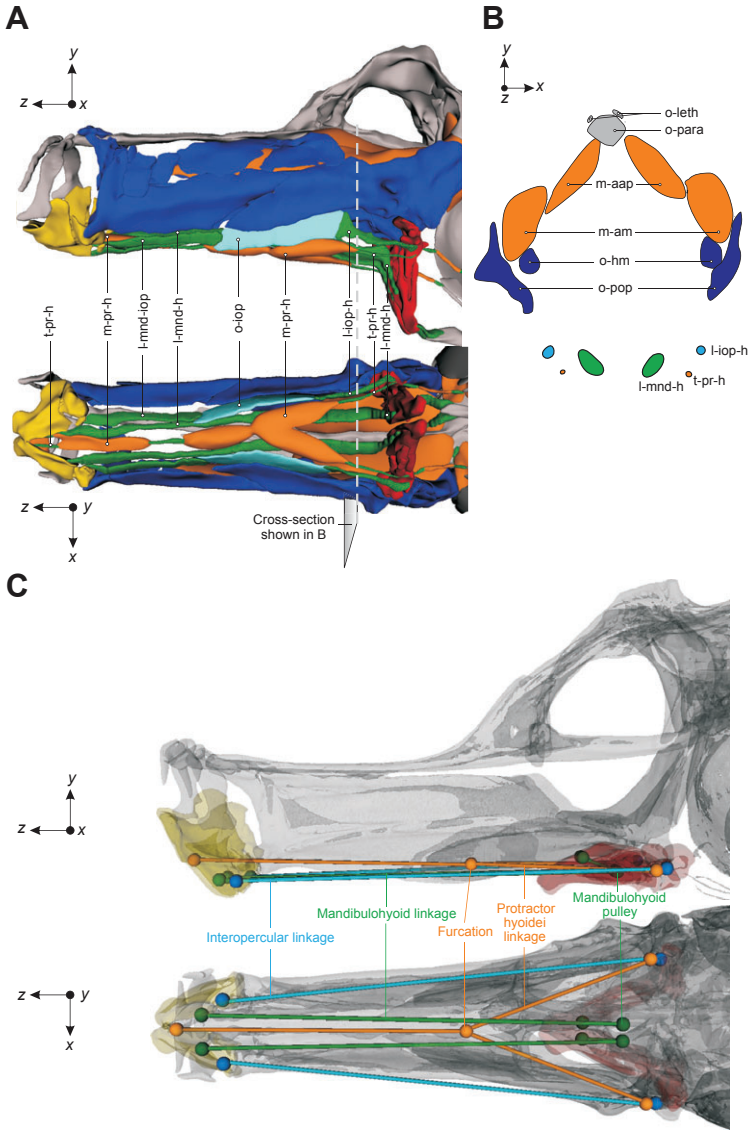

Fig. 3. Linkages between the hyoid and the lower jaw in *Hippocampus reidi*. A morphological reconstruction (A) based on serial histological sections (Leysen et al., 2011) shows the three linkages (mandibulohyoid linkage, protractor hyoidei linkage, and interopercular linkage) in lateral view, ventral view and in cross-section (B) close to the hyoid. The linkage tissues in A and B are tendon or ligament (green), muscle (orange) or bone (light blue). The modelled spring connection, including a furcation point for the protractor hyoidei linkage, and a pulley point for the mandibulohyoid linkage are illustrated in C. l-iop-h, interoperculo-hyoid ligament; l-mnd-iop, mandibulo-interopercular ligament; l-mnd-h, mandibulo-hyoid ligament; m-aap, adductor arcus palatini muscle; m-am, adductor mandibulae muscle; m-pr-h, protractor hyoidei muscle; o-hm, hyomandibular bone; o-iop, interopercular bone; o-leth, lateral ethmoid bone; o-para, parasphenoid bone; o-pop, preopercular bone; t-pr-h, protractor hyoidei tendon.

into a central muscle belly in which the left and right portions fuse. The forked central part of the protractor hyoidei is connected by an intermediate tendon with an anterior protractor hyoidei part that is elongated in shape. Finally, two thin tendons provide insertion relatively anterior on the medial side of the lower jaws, still very close to the mediosagittal plane (Fig. 3A).

The interopercular linkages are the most lateral of the three paired linkage elements. The origins of the interopercular ligaments on the ceratohyals are very close to the origins of the protractor hyoidei tendons, only slightly more posterior and more lateral. These ligaments attach to the elongated, plate-like interopercular bones. The anterior ligament insertions on the lower jaws are the most posterior and lateral of all linkages described here (Fig. 3A).

Whereas the lengths of the interopercular linkages are modelled as straight 3D lines from origin to insertion, the other two linkage pairs are modelled slightly more complexly to correspond more closely to the morphology described above. Pulley points are defined at the centre of the folding zone of the mandibulohyoid ligaments (Fig. 3C). Consequently, the length of the mandibulohyoid linkage is calculated as the sum of the length between ceratohyal origin and the pulley point, and the length between the pulley point and the lower jaw insertion. Similarly, a single furcating point is defined at the position where the protractor hyoidei muscles fuse (Fig. 3C). As a geometrical approximation that is mathematically straightforward, the positions of both pulley and furcating points are assumed to be fixed with respect to the neurocranium-bound frame of reference.

Hyoid and lower jaw kinematics

The objective of our modelling study is to perform muscle force transmission analyses with the hyoid at different positional stages as it rotates in the sagittal plane (Fig. 1). However, at certain instances during the hyoid retraction, the lower jaw rotates as well (Roos et al., 2009b). This must be taken into account, since this has an influence on the orientation and length of the hyoid-to-lower jaw linkages. To do so, the average kinematic profiles of lower jaw and hyoid rotation in *H. reidi* were used [fig. 5A from Roos et al. (Roos et al., 2009b)]. These data showed the lower jaw starting to rotate ventrally when the hyoid is at ~70 deg with respect to the snout axis, and starts closing again when the hyoid passes 110 deg (Roos et al., 2009b).

Static force transmission model

A 3D model of static force transmission from the sternohyoideus muscle to the suspensorium in *H. reidi* was implemented in Matlab Simulink 7.8.0 equipped with the SimMechanics 3.1 toolbox (The MathWorks, Natick, MA, USA). The force equilibrium equations for this multibody system are derived automatically by SimMechanics. The assumption of a static force transmission implies that there is no accelerated motion of the bodies as a result of the external forces imposed on the system. Since the later instance of hyoid retraction (3 to 20 ms) show no rotational acceleration of the hyoid (Fig. 1), and also the rate of lateral expansion of the snout is fairly constant between 5 and 15 ms (Roos et al., 2009b), a static model of force transmission is sufficient to capture the mechanics during most of the duration of suction generation in seahorses.

As input in the model, an arbitrary unit of force is exerted on the urohyal articulation with the ceratohyals along the approximate line of action of the urohyal–sternohyoideus (Fig. 2C). The presented output of the model is the torque on the left suspensorium, where positive torques are abductive (i.e. causing snout widening), and negative torques are adductive (i.e. causing snout narrowing). Since the model is bilaterally symmetric, the magnitude of the torque on the right suspensorium is equal to that on the left suspensorium.

The linkages between the hyoid and the lower jaw are modelled as linear springs that only exert force in extension. We assumed that the forces from these linkages resist rotation of the ceratohyals in the sagittal plane so that the latter stop rotating at the maximum angle observed *in vivo* [113.5 deg (Roos et al., 2009b)]. Therefore, at this time the counterclockwise torque on the hyoid (fish facing the left) by the input force must equal the sum of the clockwise torques by the three linkages. Yet, with this single assumption it is still not possible to calculate how much force dissolves into each of the three linkage pairs. Therefore, it was assumed that the maximal force exerted by each linkage is proportional to the cross-sectional areas just anterior of the hyoid (Fig. 3B). The individual linkage lengths in the model with the hyoid fully adducted (i.e. parallel with the snout axis from lateral view) were set as resting lengths (force=0). The simulations were performed for three configurations of the suspensorium planes: (1) using the position as measured from the scanned specimen, (2) a compressed snout where the suspensoria are rotated in adduction by 5 deg, and (3) an expanded snout where the suspensoria are rotated in abduction by 5 deg. Note that during all static force transmission calculations, the suspensoria are fixed in one of these positions.

Dynamic force transmission model

To evaluate the temporal aspects of the force transmitted from the hyoid to the suspensorium, a dynamical simulation was performed. The static force transmission model described above was modified so that the ceratohyals are free to rotate posteriorly from their starting positions (Fig. 2) due to a retraction force exerted on the hyoid tip (the lower jaw and suspensorium are still fixed). By using a realistic moment of inertia of the hyoid for rotation in the sagittal plane, and a realistic input force, it is possible to model *in vivo* hyoid rotation kinematics (Roos et al., 2009b).

The moment of inertia of the hyoid for rotation in the sagittal plane was estimated by modelling the hyoid as a half-spheroid with a length (c) of 7 mm, a width radius (b) of 3.5 mm and a height radius (a) of 1.2 mm. These dimensions were measured on the CT-scan reconstruction (Fig. 2). Assuming the spheroid to be filled with water (density ρ=1000 kg m^{-3}), its mass M (including both halves) can be calculated as:

$$M = \frac{3}{4}\rho\pi abc\ , \qquad (1)$$

and the hyoid moment of inertia for rotation about the left–right axis through the width radius b (I_{xx}) by:

$$I_{xx} = \frac{1}{5}M(b^2 + c^2)\ . \qquad (2)$$

A hyoid mass of ½M (46.2 mg), and ½I_{xx} (5.66×10^{-10} kg m^2) were used as inertial properties in the model.

The sternohyoideus–hypaxial muscle complex consists of a left and right portion. Posterior to the point of their fusion (close to the urohyal), these two portions diverge from each other at an angle of approximately 30 deg. The muscle has a multipennate architecture (Fig. 4) with central tendons for both the sternohyoid and hypaxial parts. Dissection and stereomicroscopy (Leica M165C, Leica Microsystems, Wetzlar, Germany) showed that this muscle has an average fibre length of 2.49 mm and an average angle of pennation (ϕ) of 21 deg. It weighs 25.4 mg in a specimen with a head length of 20.2 mm. Consequently, assuming a density (ρ) of 1000 kg m^{-3}, the physiological cross-sectional area (PCSA) of this muscle [PCSA=(muscle mass×cosϕ)/(ρ×fibre length)] approximates 9.52 mm^2. If we assume that this muscle is capable of producing a peak isometric tetanus force of 200 kN m^{-2} (Van Wassenbergh et al., 2007b), a typical value for catfish cranial muscle, then peak isometric force is estimated to be 1.9 N.

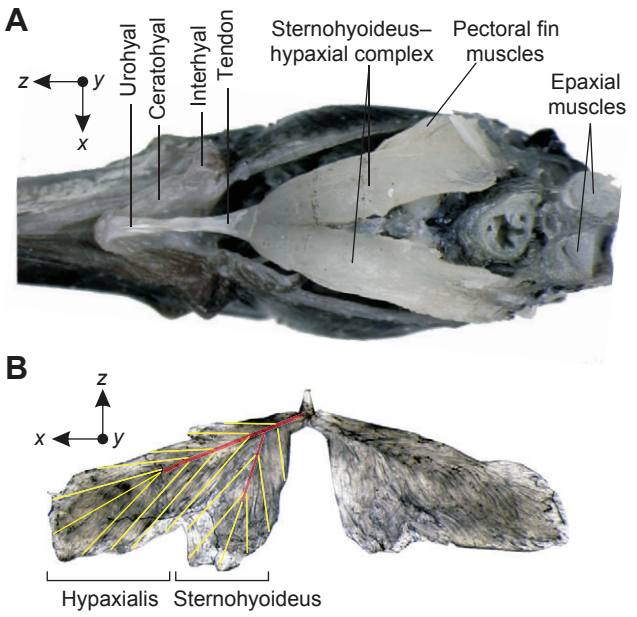

Fig. 4. Morphology of the hyoid retractor muscle–tendon system. (A) A ventral view on the posterior head region after removing the opercular and branchiostegal cover shows the hyoid (urohyal, ceratohyal and interhyal) connected *via* a relatively long tendon to the muscle complex bilaterally composed of a sternohyoideus part (origin on the pectoral girdle) and a hypaxial part (origin on the medial side of the lateral bony cover plates). (B) Spreading this muscle complex shows a multipennate structure, with a central tendon (red lines) in both the sternohyoideus and hypaxial parts. The approximate muscle fibre orientations and lengths used to calculate the physiological cross-sectional area (see Materials and methods) are drawn (yellow lines). Scale bar, 5 mm.

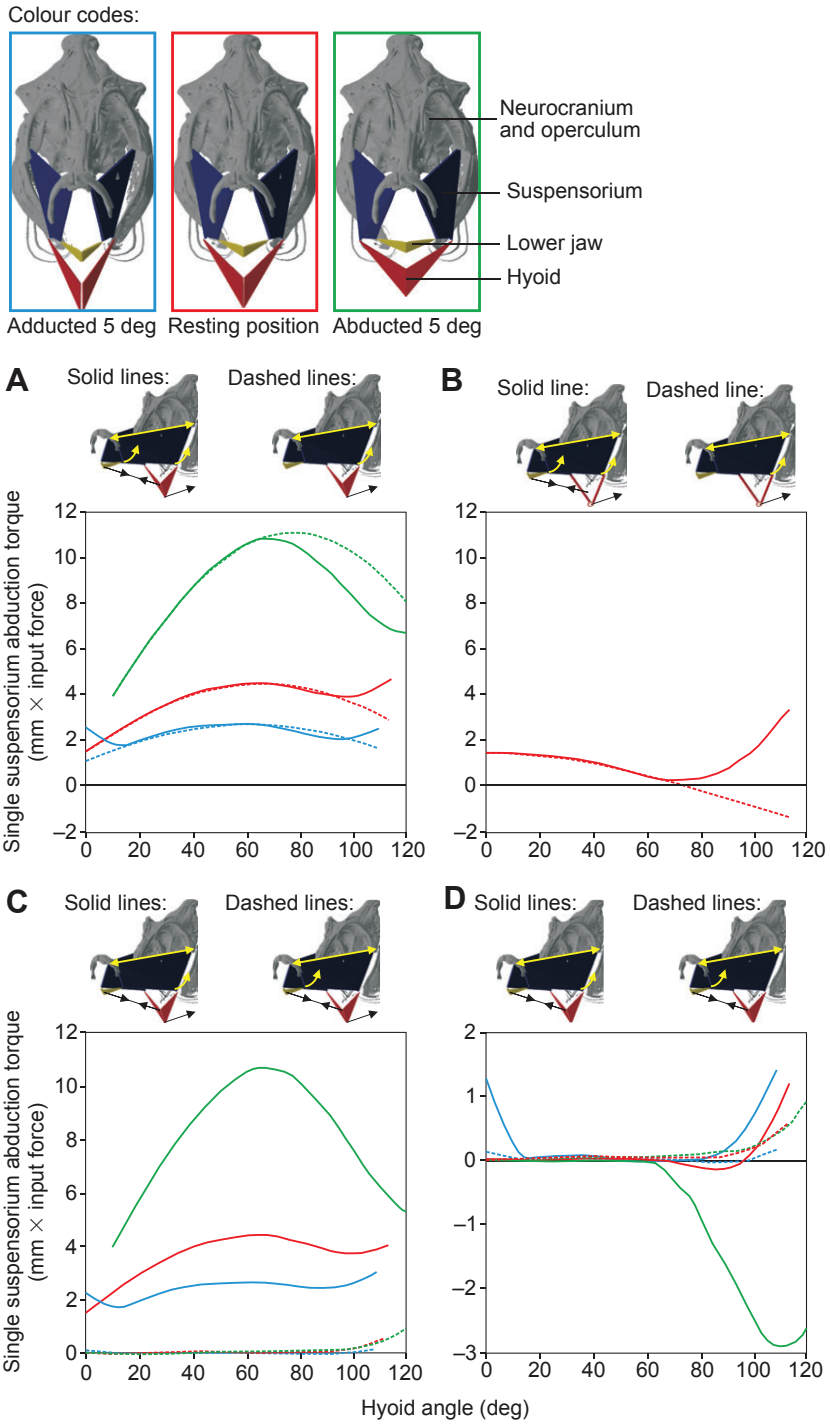

Fig. 5. Static force transmission to suspensorium abduction for a range of hyoid retraction positions (*x*-axis), and for three suspensorium angles (5 deg adducted, blue curves; resting position, red curves; 5 deg abducted, green curves; see frontal view illustrations at the top). The full model results are shown in A (solid lines), to which hypothetical models without the connections to the lower jaw can be compared (dashed lines). In B, the ceratohyal hinge joint is replaced by a spherical joint at the distal tip of the hyoid, also showing a full model (solid line) and a model without elastic connections to the lower jaw (dashed line). In C, the suspensorium torque is separated in a component caused by reaction forces at the interhyal–preopercular joint (solid lines), and the part caused by the reaction forces at the quadrate–mandibular joint (dashed lines). In D, model output without the direct effect of the input force (only by tension in the hyoid-to-lower jaw linkages) is shown for suspensorium abduction at the interhyal–preopercular joint (solid lines) and at the quadrate–mandibular joint (dashed lines).

The dynamic force input generated by the sternohyoideus–hypaxial muscle–tendon system, of which the serial elastic component is almost certainly loaded prior to the onset of hyoid retraction (Van Wassenbergh et al., 2008), is very difficult to predict without knowledge on the *in vivo* strain of the tendons and muscle fibres. A first simulation was performed with, for reasons of simplicity, a constant hyoid retraction force input of 1.9 N (the theoretical maximum isometric force as calculated above). However, it is likely that the hyoid retraction force will drop from this initial value due to tendon recoil, but will rise again to a similar value when the hyoid retraction is halted and the muscle fibers regain an isometric contraction state (at shorter fibre lengths, but fibres are assumed still to work at the plateau of the force–length relationship). Therefore, a second simulation was performed in which the force input first drops to an arbitrary value of zero at a hyoid angle of 45 deg (just prior to tension building in the linkages to the lower jaw), and then rises again to its isometric contraction maximum of 1.9 N at the observed static equilibrium for hyoid retraction at 113.5 deg. This simulation illustrates a reduced force input due to tendon recoil, which can be expected for the intermediate phase (i.e. during quick hyoid retraction).

Since the linear spring stiffness constants used for the linkages between the hyoid and the lower jaw in the static force transmission model would only cause deceleration of the rotation

of the hyoid starting at the observed maximum angle (i.e. 113.5 deg), spring stiffness values had to be increased by a certain factor in the dynamical models. Running several simulations showed that a factor of 2.05 was sufficient to reach a zero hyoid rotation velocity at 113.5 deg for the constant force simulation. No spring stiffness adjustments were needed for the case with the variable force input (second simulation described above). The recoil phase that inevitably follows the loading of these springs will not be considered.

RESULTS

Static model

For the entire range of simulated hyoid and lower jaw positions in the static force transmission model of buccopharyngeal widening in *H. reidi*, the forces acting on the hyoid and lower jaw always resulted in suspensorial abduction (Fig. 5A; positive suspensorium torque). These forces are the sternohyoideus input force (Fig. 2C), and at large hyoid angles also the forces imposed by the linkages between the hyoid and the lower jaw (Fig. 3C). However, the magnitude of the forces transmitted to the suspensorium strongly depended on its abduction–adduction state: higher suspensorium abduction torques were calculated at more abducted positions (Fig. 5A,C). In theory, the reaction forces at the articulation between interhyal and the suspensorium will approach an infinite value when the hyoid bars become fully unfolded (i.e. when the hyoid symphysis hinge axis intersects the axis for sagittal plane hyoid rotation) (see also Aerts, 1991).

For the model with the suspensorium in its resting position, the highest suspensorium abduction torque is reached at the most retracted hyoid angle (113.5 deg). At this position, the hyoid-to-lower jaw linkages are stretched the most and exert the highest forces in our simulation. Compared with the model with only the sternohyoideus input force, a positive influence of tension in these ligaments on suction force transmission occurs at hyoid angles beyond 90 deg (Fig. 5A,C). The maximal torques on a single suspensorium in the static force transmission model were 2.7, 4.6 and 10.7 mm × input force for the −5, 0 and +5 deg abducted suspensoria models, respectively.

The model shows an important role of the hinge joint between the ceratohyals (Fig. 5). Replacing this joint by a spherical joint resulted in a reduced force transmission performance in all of the simulated hyoid and lower jaw positions: suspensorium torque starts at a similar value compared to the hinge joint simulation at 0 deg hyoid angle, but drops to only 6% at 71 deg, after which it rises again to 71% at 113.5 deg (Fig. 5B). Note that positive abduction torques by retraction of a hyoid with a spherical joint at its symphysis would only be possible at hyoid angles higher than 90 deg due to the couples of forces including the resistance from the linkages to the lower jaw: without these linkages, the input force was predicted to cause adduction for hyoid angles above 75 deg.

Suspensorium abduction torque was predominantly generated *via* the interhyal–preopercular joint (Fig. 5C). The lengths of the hyoid-to-lower jaw linkages remained very close to (or sometimes even shorter than) their original length (hyoid at 0 deg and lower jaw at −17 deg) when the hyoid was at angles lower than 70 deg. For hyoid angles higher than 70 deg, the linkage forces, and their contribution to suspensorium torque, increased towards the most retracted hyoid position (Fig. 5C). The force exerted on the lower jaw resulted in reaction forces at the quadratomandibular joint, which caused a suspensorium torque that will result in abduction. However, the magnitude of this torque delivered *via* the quadratomandibular joint is maximally 16% of the total torque (for the +5 deg suspensorium model at 113.5 deg hyoid angle), and was thus considerably lower than the torque delivered *via* the interhyal–preopercular joint. The model also calculated that the force of the hyoid-to-lower jaw linkages transmitted to suspensorium torque was higher in magnitude *via* the interhyal–preopercular joint than *via* the quadratomandibular joint (Fig. 5D).

The main contribution to suspensorium abduction torque was generated by the input force vector (sternohyoideus–hypaxial force), followed by the mandibulohyoid ligament (Fig. 6) for the model with the maximally retracted hyoid. This hyoid position corresponds to the phase where the static force equilibrium is most closely approximated *in vivo* and most of the work for generating suction is being done (Fig. 1). The contribution of the other two elements in the model, the interopercular linkage and the protractor hyoidei linkage, was negligible. The protractor hyoidei force even had an inverse effect: it causes a relatively small amount of adduction at the interhyal joint (but abduction at the quadratomandibular joint). The dominant element of the three hyoid-to-lower jaw linkages, the mandibulohyoid ligament, outperformed the other two elements in causing abduction torque at both joints with the suspensorium (Fig. 6).

Dynamic model

The dynamic models showed a steeper increase in the force transmitted to the suspensorium at the higher range of hyoid angles (Fig. 7) compared to the static force transmission models (Fig. 5). The maximum single suspensorium torque when the hyoid reaches a standstill position at 113.5 deg was 7.2 mm × input force in the model with the constant hyoid retraction input force (Fig. 7A). This is considerably higher than calculated with the static model (4.6 mm

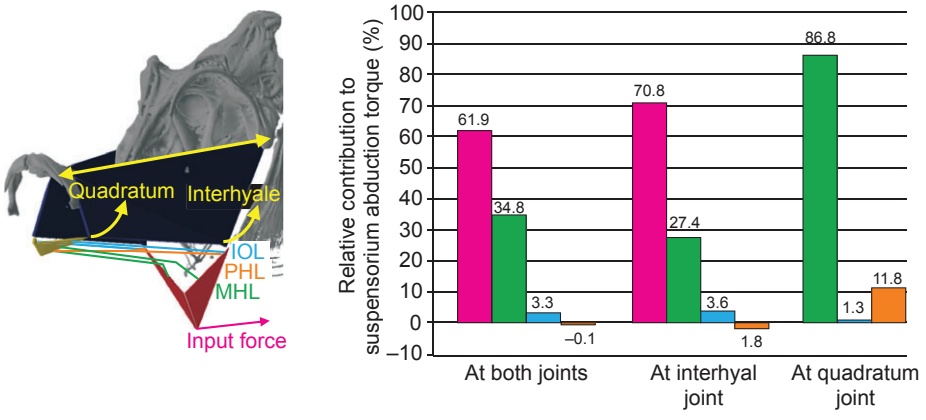

Fig. 6. The relative contributions to suspensorium abduction torque (at 113.5 deg retracted hyoid) of the four muscle, tendon or ligament components in the static force transmission model (input force, pink; mandibulohyoid ligament MHL, green; interopercular linkage IOL, blue; protractor hyoidei linkage PHL, orange).

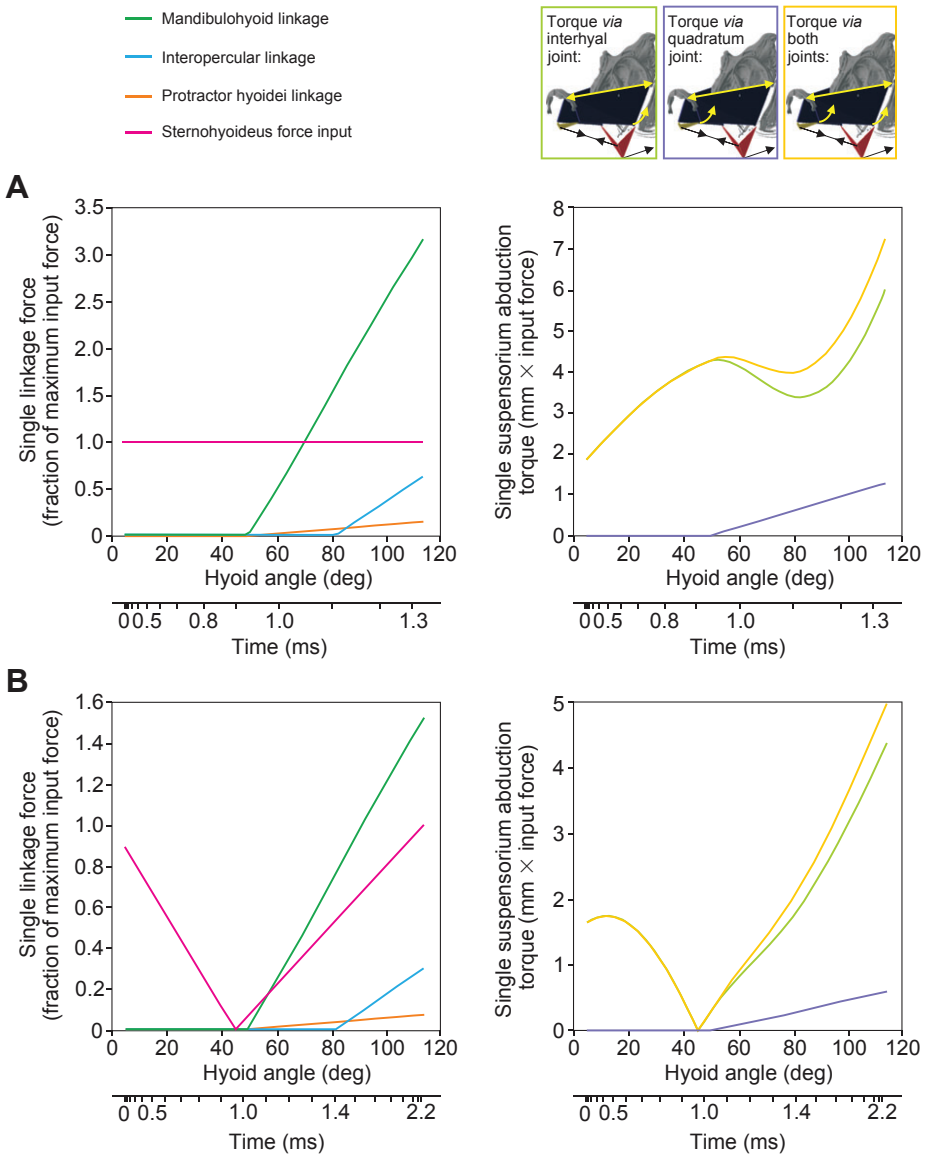

Fig. 7. Results of the dynamic force transmission models with (A) a constant force input, and (B) a force input decreasing during the quick hyoid rotation phase to mimic an elastic recoil behaviour of the sternohyoid–hypaxial tendons. The forces exerted by the different components in the system are shown in the left-hand column, the torque on a single suspensorium is displayed in the right-hand column (colour codes explained above each column). Note the drop in suspensorium torque coinciding with the early drop in input force, and the considerable steeper increase in suspensorium torque at high hyoid angles compared with the static force transmission model (Fig. 5A).

× input force; solid red curve in Fig. 5A). This tendency (i.e. a steeper increase in force transmission at large hyoid angles) is even more pronounced when including a drop in force to mimic the effect of recoil of the pre-loaded sternohyoideus tendon (Fig. 7B). In the latter simulation, the early peak in force transmission to the suspensorium at a hyoid angle of about 60 deg (Figs 5, 6) was no longer present. The peak suspensorium torque calculated for this model was 5.0 mm × input force.

DISCUSSION

Snout widening *via* forces imposed on the hyoid and lower jaw

Our study aimed at understanding how suction force is generated in the seahorse *H. reidi*, which served as a model species for the fishes of the family Syngnathidae. In contrast to most other fish, syngnathids produce suction almost exclusively by abduction of the suspensoria, which border the lateral side of their relatively long snout (Roos et al., 2009b). Previous work dealing with the mechanics of suspensorial abduction in non-syngnathid percomorph fishes hypothesized that suspensorial abduction is mainly caused by the left and right hyoid bars that push laterally on the medial side of the suspensoria, when the tip of the hyoid is being retracted posteriorly by the sternohyoideus muscle (Muller, 1989; Aerts, 1991; De Visser and Barel, 1996). The high magnitudes of suspensorium abduction torques calculated here by mathematical modelling (~5 mm × input force on each of the suspensoria; Figs 5, 7) confirm this hypothesis for our model species. For the levator arcus palatini muscle of a single side of the head to generate this amount of torque on a suspensorium, its physiological cross-sectional area would have to at least equal that of the entire sternohyoideus–hypaxial muscle complex (Fig. 4) assuming that it attaches perpendicularly to the most ventral point on the suspensorium (~5 mm radius to the suspensorium hinge axis). A recent morphological study showed that the levator arcus palatini is much smaller than the sternohyoideus, inserts approximately halfway the distance from the suspensorium hinge axis, and is far from perpendicular to the suspensorium plane in *H. reidi* (Leysen et al., 2011). Consequently, our data confirm that forceful suspensorial abduction during suction feeding in *H. reidi* results from hyoid retraction, whereas the role of the levator arcus palatini is probably limited to powering slow movements of the suspensoria during respiration.

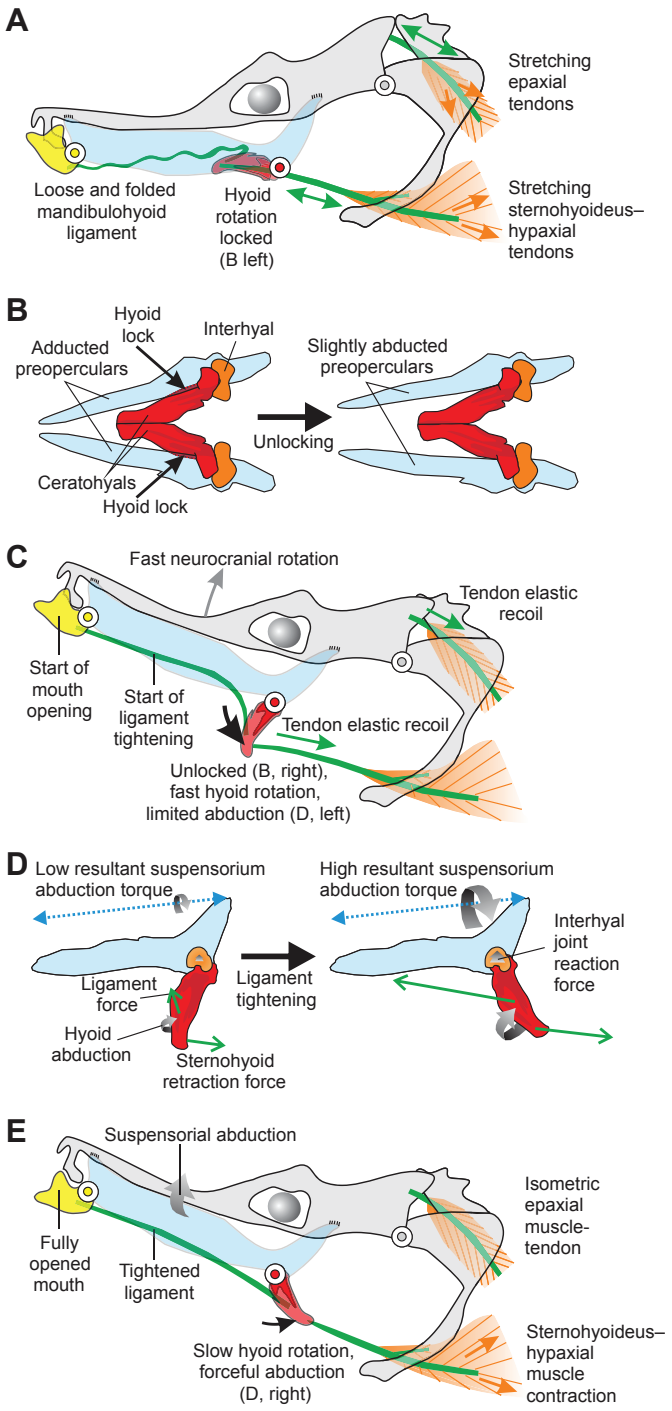

Fig. 8. Schematic illustration of hypotheses emanating from this study and previous work on the mechanics involved in the consecutive phases of prey-capture in seahorses. The figure is simplified by showing only the most important linkage pair between the hyoid and the lower jaw (i.e. the mandibulohyoid ligaments). Circles represent the three skeletal joints allowing rotation in the sagittal plane (occipital joint, grey; interhyal–preopercular joint, red; quadratomandibular joint, yellow). During the preparatory phase (A), the epaxial muscles and very probably also the sternohyoideus–hypaxial muscles contract (Muller, 1987; Van Wassenbergh et al., 2008). Because the hyoid is prevented from rotating ventrally at this stage, these two muscle groups work antagonistically, and their tendons are stretched without causing any skeletal motion. The locking of the hyoid (B; ventral view) is hypothesized to be caused by a small ventromedial part of the adducted preopercular bones lying ventral of the lateral sides of the posterior ceratohyals (B, left) (de Lussanet and Muller, 2007). Relaxation of the adductor arcus palatini muscles would then allow the ceratohyals to pass ventrally in between the left and right preopercular bones (B, right). This unlocking of the hyoid simultaneously causes explosively fast rotations of the neurocranium and the ceratohyals driven by elastic recoil of the pre-loaded, post-cranial tendons (C). The dorsal rotation of the neurocranium and the ventral rotation of the hyoid are coupled in a system that can be modelled as a planar four-bar chain (Muller, 1987; Flammang et al., 2009; Roos et al., 2009a). During this head-rotation phase, the ceratohyals can freely rotate due to the initially loose and folded nature of the mandibulohyoid ligament (i.e. the resting position, see A). This ligament starts building up stress, causing onset of mouth opening from the time when the hyoid passes an angle of about 80 deg with respect to the snout. At this time, the gradually increasing stress in the mandibulohyoid ligament causes laterally directed reaction forces at the interhyal–preopercular joints (D; lateral view after removing the left preoperculum) (Figs 5, 7). These forces cause the suspensoria to abduct, resulting in snout widening, which initiates the phase of suction generation (E). The hyoid now rotates very slowly (Fig. 1), and the neurocranium is approximately stationary (Roos et al., 2009b). The mouth is fully opened by the posterior forces from the linkages with the hyoid (Fig. 1). Nearly all work for suction is generated during this phase *via* forces exerted on the hyoid, assisted by a limited amount of forces transmitted *via* the lower jaw.

Our study is the first to show that force transmitted *via* the lower jaws also contributes to lateral expansion of the head during suction feeding. However, its contribution was estimated to be relatively small (generally less than 10%) compared with the suspensorium torques generated at the level of the hyoid. Yet, it should be noted that our model did not include the forces by the adductor mandibulae muscles on the lower jaws, which can have an effect on the results for the large hyoid angles (>90 deg) since lower jaw closing was observed *in vivo* during this period (Roos et al., 2009b).

Importance of the interceratohyal hinge joint

We hypothesized that the hyoid symphysis will function as a hinge joint in *H. reidi*, rather than as a spherical (or ball-and-socket) joint, because of the posteriorly pointing tip of the hyoid at the moment of suspensorium abduction (Fig. 1). Morphological data showed that the medial sides of the ceratohyals indeed resemble a hinge joint (Fig. 2D). A previous study found the same type of joint in the pipefish *Syngnathus acus* (de Lussanet and Muller, 2007). Our force transmission models showed that the hinge joint of *H. reidi* allows high force transmission to the suspensoria for a wider range of hyoid angles in the sagittal plane compared with a spherical joint at the hyoid tip (Fig. 5). The hinge joint between the two hyoid bars therefore prevents a torque reversal (causing adduction instead of abduction), a problematic situation that can occur with a spherical joint at largely retracted hyoid angles (Fig. 5B).

However, the presence of a hinge joint at the hyoid symphysis does not explain why the hyoid rotates over a much larger angle in Syngnathidae compared with other suction-feeding fishes. Cichlid fishes, for example, also have this interhyoid hinge joint (Aerts, 1991) but sagittal plane rotations of the hyoid are limited [46 deg (De Visser and Barel, 1998)] compared with syngnathid fishes [up to 160 deg (Roos et al., 2009b)]. We identified two reasons for this remarkable difference and discuss them below.

Hyoid function and timing of suction generation in syngnathids *versus* generalized fish

A first fundamental difference is that in more generalized suction feeders such as cichlids the hyoid fulfils its role in ventral expansion during suction feeding: ventral rotation of the hyoid tip pushes the floor of the buccal cavity away from the roof of the buccal cavity

(e.g. Sanford and Wainwright, 2002). This function could not be demonstrated for the rotation of the small hyoid of *H. reidi* (Roos et al., 2009b). Consequently, this important constraint on the range of sagittal plane hyoid angles from which suspensorium abduction must be generated is no longer present in syngnathid fishes.

A second fundamental difference is related to the timing of suction generation. Suction feeding in syngnathiform fishes is generally referred to as pivot feeding to indicate the crucial role of dorsal rotation of the head during feeding (de Lussanet and Muller, 2007; Van Wassenbergh et al., 2011). By rotating the long snout, the distance between the small mouth and the prey is bridged in only a few milliseconds. Although most non-syngnathiform fishes also show dorsal rotation of the neurocranium during suction feeding (e.g. Gibb and Ferry-Graham, 2005), they generate suction while the neurocranium is rotated. It was shown that the volume of the head of *H. reidi* starts to increase 3.5 ms after the start of cranial rotation (Roos et al., 2009b). At this instant, the head has already reached its final, elevated position by which the mouth is brought close to the prey. Because head rotation is mechanically coupled with sagittal plane hyoid rotation in generalized teleost fishes [planar four-bar linkage model (Muller, 1987)], the hyoid must rotate for some time to allow a certain amount of cranial rotation.

In order not to waste energy in suction generation when the mouth is still too far away from the prey for suction to have an effect, the first milliseconds of hyoid retraction should ideally occur without performing suspensorium abduction work (Roos et al., 2009b). Our analysis showed that a free rotation of the hyoid caused by recoil of the sternohyoideus tendon, without a counterforce by the linkages to the lower jaw, can provide this function (Fig. 7B). Next, when tension builds in the hyoid-to-lower jaw linkages, sagittal plane hyoid and head rotation will be halted (again by the four-bar coupling between both elements), and there will be high force transmission for suspensorium abduction. Such a system will automatically start generating suction with the appropriate timing for a pivot feeder (i.e. during and after the deceleration of cranial rotation). A summary of the crucial mechanical events during different stages of prey capture in syngnathid pivot feeders is given in Fig. 8.

Snout widening continues for a considerable time (>15 ms) during which there is a very slow hyoid retraction in seahorses (Fig. 1). This sustained retraction indicates that, after the elastic recoil phase of the sternohyoideus tendon that causes the quick hyoid rotation, the sternohyoideus–hypaxial muscle (as well as the epaxial muscles causing cranial dorsorotation) must be producing force. In some individuals of the species *Hippocampus abdominalis* and *Syngnathus leptorhynchus*, a dual-phase hyoid and cranial rotation was observed in some individuals (S.V.W., unpublished observations). This is probably caused by a short time delay between the drop in force after elastic recoil and the building of active muscle force from the sternohyoideus–hypaxial muscle complex.

Function of the hyoid-to-lower jaw linkages

The mechanism described above shows a crucial role for the linkages between the hyoid and the lower jaw for transmitting suction force in *H. reidi*. However, since this species has three separate linkage pairs between hyoid and lower jaw (Fig. 3), the precise function of each of these linkages remains unclear. A similar linkage configuration was also found in the pipefishes *Syngnathus acus* (Branch, 1966) and *Dunckerocampus dactyliophorus* (Leysen et al., 2011). Our analysis showed that the linkage with the largest cross-sectional area at the connection with the hyoid, the mandibulohyoid ligament, is mainly responsible for the critical force transmission during suction feeding (Fig. 6). When the hyoid of *H. reidi* is in its resting position (i.e. tip pointing towards the mouth), the mandibulohyoid ligament is folded at the level of the hyoid base (Fig. 3A, Fig. 8A). Consequently, this ligament will only be stretched at highly retracted hyoid positions as displayed during suction feeding, and not during the low-magnitude hyoid rotation of respiration. Its function is therefore probably reserved to force transmission during suction feeding.

The interopercular linkage can theoretically fulfil the same role as the mandibulohyoid ligament in contributing to suspensorium abduction torque (Fig. 6). However, as a consequence of its thin cross-sectional area (Fig. 6B), and its specific line of action (Fig. 6C), our model predicted that this ligament only plays a negligible role in this process. Given that this linkage is the most lateral of the three linkages, and consists of the long and flat interopercular bone connected *via* ligaments to the hyoid and lower jaw (Fig. 3A), we hypothesize that its main function is to support the ventrolateral skin from collapsing inward due to the sub-ambient intrabuccal pressure generated during suction.

Force from the protractor hyoidei linkage, which has a peculiar forked shape (Fig. 3A) and is the thinnest tendon of the three linkages (Fig. 3B), is predicted to cause a very limited amount of adduction of the suspensorium (Fig. 6). Consequently, a role in transmitting force to generate suction can be excluded for this muscle–tendon complex. Because of its inverse action on the suspensorium, we hypothesize that its function in *H. reidi* is limited to what its name suggests: protracting the hyoid and helping in recovering the suspensorium to its resting position. Yet, as shown for other teleost fishes (Van Wassenbergh et al., 2005), an important role for this muscle in mouth opening is also possible.

Conclusions

Our analyses illustrate that the complex functional morphology of the feeding apparatus in syngnathid fishes is better understood with the help from mathematical modelling of the mechanics involved. Previous work identified a novel mechanism of elastic energy storage and release to amplify power for the dorsal rotation of the head and snout when striking at prey (Muller, 1987; Van Wassenbergh et al., 2008) (Fig. 8). We have now shown how the feeding mechanics in syngnathids are modified, relative to generalized suction-feeding percomorphs, to generate forceful suction with a delay in timing with respect to the dorsal rotation of the head and snout, which is unique among fishes.

ACKNOWLEDGEMENTS

We thank the two anonymous reviewers for their help in improving this article.

FUNDING

S.V.W. is postdoctoral fellow of the Fund for Scientific Research, Flanders. This work was supported by a grant from the Fund for Scientific Research, Flanders (G053907 to D.A. and P.A.).

REFERENCES

Adriaens, D., Baskin, J. N. and Coppens, H. (2010). Evolutionary morphology of trichomycterid catfishes: about hanging on and digging in. In *Origin and Phylogenetic Interrelationships of Teleosts: Honoring Gloria Arratia: Proceedings of the International Symposium at the ASIH Annual Meeting in St Louis, Missouri, 2007* (ed. J. S. Nelson, H.-P. Schultze, M. V. H. Wilson and G. A. Fuentes), pp. 337-362. München: Verlag Dr. Friedrich Pfeil.

Aerts, P. (1991). Hyoid morphology and movements relative to abducting forces during feeding in *Astatotilapia elegans* (Teleostei: Cichlidae). *J. Morphol.* **208**, 323-346.

Aerts, P. and Verraes, W. (1991). Force transmission from hyoid to suspensorium during feeding in *Astatotilapia elegans*: a form-function relationship. *Ann. Kon. Mus. Mid. Afr. Zool. Wetensch.* **262**, 81-84.

Aerts, P., Osse, J. W. M. and Verraes, W. (1987). A model of jaw depression during feeding in *Astatotilapia elegans* (Teleostei: Cichlidae): Mechanisms for energy storage and triggering. *J. Morphol.* **194**, 85-109.

Branch, G. M. (1966). Contributions to the functional morphology of fishes. Part III. The feeding mechanism of *Syngnathus acus* Linnaeus. *Zool. Afr.* **2**, 69-89.
de Lussanet, M. H. C. and Muller, M. (2007). The smaller your mouth, the longer your snout: predicting the snout length of *Syngnathus acus*, *Centriscus scutatus* and other pipette feeders. *J. R. Soc. Interface* **4**, 561-573.
De Visser, J. and Barel, C. D. N. (1996). Architectonic constraints on the hyoid's optimal starting position for suction feeding of fish. *J. Morphol.* **228**, 1-18.
De Visser, J. and Barel, C. D. N. (1998). The expansion apparatus in fish heads, a 3-D kinetic deduction. *Neth. J. Zool.* **48**, 361-395.
Diogo, R. (2005). *Morphological Evolution, Aptations, Homoplasies, Constraints and Evolutionary Trends: Catfishes as a Case Study on General Phylogeny and Macroevolution.* Enfield, NH: Science Publishers.
Ferry-Graham, L. A. and Konow, N. (2010). The intramandibular joint in *Girella*: a mechanism for increased force production? *J. Morphol.* **271**, 271-279.
Flammang, B. E., Ferry-Graham, L. A., Rinewalt, C., Ardizzone, D., Davis, C. and Trejo, T. (2009). Prey capture kinematics and four-bar linkages in the bay pipefish, *Syngnathus leptorhynchus*. *Zoology* **112**, 86-96.
Gibb, A. C. and Ferry-Graham, L. (2005). Cranial movements during suction feeding in teleost fishes: are they modified to enhance suction production? *Zoology* **108**, 141-153.
Gregory, W. K. (2002). *Fish Skulls: a Study of the Evolution of Natural Mechanisms.* Malabar, FL: Krieger Publishing Company.
Konow, N., Bellwood, D. R., Wainwright, P. C. and Kerr, A. M. (2008). Evolution of novel jaw joints promote trophic diversity in coral reef fishes. *Biol. J. Linn. Soc. Lond.* **93**, 545-555.
Leysen, H., Jouk, P., Brunain, M., Christiaens, J. and Adriaens, D. (2010). Cranial architecture of tube-snouted Gasterosteiformes (*Syngnathus rostellatus* and *Hippocampus capensis*). *J. Morphol.* **271**, 255-270.
Leysen, H., Christiaens, J., De Kegel, B., Boone, M. N., Van Hoorebeke, L. and Adriaens, D. (2011). Musculoskeletal structure of the feeding system and implications of snout elongation in *Hippocampus reidi* and *Dunckerocampus dactyliophorus*. *J. Fish Biol.* **78**, 1799-1823.
Muller, M. (1987). Optimization principles applied to the mechanism of neurocranial levation and mouth bottom depression in bony fishes (Halecostomi). *J. Theor. Biol.* **126**, 343-368.
Muller, M. (1989). A quantitative theory of expected volume changes of the mouth during feeding in teleost fishes. *J. Zool.* **217**, 639-662.
Muller, M. (1996). A novel classification of planar four-bar linkages and its application to the mechanical analysis of animal systems. *Philos. Trans. R. Soc. Lond. B* **351**, 689-720.
Roos, G., Leysen, H., Van Wassenbergh, S., Herrel, A., Jacobs, P., Dierick, M., Aerts, P. and Adriaens, D. (2009a). Linking morphology and motion: a test of a four-bar mechanism in seahorses. *Physiol. Biochem. Zool.* **82**, 7-19.
Roos, G., Van Wassenbergh, S., Herrel, A. and Aerts, P. (2009b). Kinematics of suction feeding in the seahorse *Hippocampus reidi*. *J. Exp. Biol.* **212**, 3490-3498.
Sanford, C. P. J. and Wainwright, P. C. (2002). Use of sonomicrometry demonstrates the link between prey capture kinematics and suction pressure in largemouth bass. *J. Exp. Biol.* **205**, 3445-3457.
Van Wassenbergh, S. and Aerts, P. (2008). Rapid pivot feeding in pipefish: flow effects on prey and evaluation of simple dynamic modelling via computational fluid dynamics. *J. R. Soc. Interface* **5**, 1291-1301.
Van Wassenbergh, S., Herrel, A., Adriaens, D. and Aerts, P. (2005). A test of mouth-opening and hyoid-depression mechanisms during prey capture in a catfish using high-speed cineradiography. *J. Exp. Biol.* **208**, 4627-4639.
Van Wassenbergh, S., Herrel, A., Adriaens, D. and Aerts, P. (2007a). No trade-off between biting and suction feeding performance in clariid catfishes. *J. Exp. Biol.* **210**, 27-36.
Van Wassenbergh, S., Herrel, A., James, R. S. and Aerts, P. (2007b). Scaling of contractile properties of catfish feeding muscles. *J. Exp. Biol.* **210**, 1183-1193.
Van Wassenbergh, S., Strother, J. A., Flammang, B. E., Ferry-Graham, L. A. and Aerts, P. (2008). Extremely fast prey capture in pipefish is powered by elastic recoil. *J. R. Soc. Interface* **5**, 285-296.
Van Wassenbergh, S., Roos, G. and Ferry, L. (2011). An adaptive explanation for the horse-like shape of seahorses. *Nat. Commun.* **2**, 164.
Vial, C. I. and Ojeda, F. P. (1992). Comparative analysis of head morphology of Pacific temperate kyphosid fishes: a morpho-functional approach to prey-capture mechanisms. *Rev. Chil. Hist. Nat.* **65**, 471-483.
Waltzek, T. B. and Wainwright, P. C. (2003). Functional morphology of extreme jaw protrusion in neotropical cichlids. *J. Morphol.* **257**, 96-106.
Westneat, M. W. (1994). Transmission of force and velocity in the feeding mechanism of labrid fishes (Teleostei, Perciformes). *Zoomorphology* **114**, 103-118.